

Spin-free exact two-component linear response coupled cluster theory for estimation of frequency-dependent second-order property

Sudipta Chakraborty^a, Tamoghna Mukhopadhyay^a and Achintya Kumar Dutta^{*,a}

^aDepartment of Chemistry, Indian Institute of Technology Bombay, Mumbai 400076, India

We have presented the theory, implementation, and benchmark results for spin-free exact two-component (SFX2C) linear response coupled cluster (LRCCSD) theory for static and dynamic polarizabilities of atoms and molecules. The resolution of identity (RI) approximation for two-electron integrals has been used to reduce the computational cost of the calculation and has been shown to have a negligible effect on accuracy. The calculated static and dynamic polarizability values agree very well with the more expensive X2C-LR-CCSD results. Our calculated results show that accurate predictions of polarizabilities of atoms and molecules containing heavy atoms require the use of a large basis set containing an adequate number of diffuse functions, in addition to accounting for electron correlation and relativistic effects.

**achintya@chem.iitb.ac.in*

1. Introduction

The atomic and molecular response properties in the presence of external fields (electric or magnetic) stand as a cornerstone for studying linear and nonlinear optical phenomena. Its significance spans a wide spectrum of applications, impacting fields from drug and catalysis design to the optimal functioning of optoelectronic devices such as sensors, light-emitting diodes, and piezoelectric materials. Quantum mechanical calculations of polarizabilities involve determining induced polarization as a function of the applied electric field. This is achieved through a time-independent or time-dependent perturbation calculation that accounts for the interaction between light and matter. In the last few decades, significant progress has been reported in *ab initio* calculation of response properties calculation^{1–12}. However, most of them are formulated in a nonrelativistic picture. In heavy elements, the influence of relativistic effects on response properties becomes increasingly pronounced. These relativistic effects can dramatically affect the electronic structure, leading to deviations from the predictions obtained from nonrelativistic quantum mechanical calculations. The incorporation of relativistic effects in wavefunction based calculations at the mean-field level is made possible by the implementation of the Dirac-Hartree-Fock (DHF)¹³ method, which generally relies on a four-component Dirac Coulomb Hamiltonian. The static and dynamic polarizability calculations using coupled perturbed DHF have been reported in the literature¹⁴. However, electron correlation effects have a significant contribution to the accuracy of the polarizability values¹⁵ for the nonrelativistic case. Four-component Density Functional Theory (4c-DFT)¹⁶ offers a computationally efficient way to incorporate correlation effects into the relativistic polarizability calculation. However, similar to its nonrelativistic analog, the accuracy of the relativistic DFT results is strongly dependent upon the used exchange-correlation functional and there is no systematic way to improve it^{17,18}. Wave function based electron correlation methods lead to higher accuracies in calculated polarizability values. Among the various wavefunction-based electron correlation methods, the coupled cluster method is considered to be highly accurate and systematically improvable¹⁹. Recently, Gomes and co-workers have implemented a linear response method based on a two-component relativistic Hamiltonian for polarizability and other second-order properties²⁰.

The coupled cluster^{21,22} method is known for its high computational cost and scales as iterative $O(N^6)$ power of the basis set even at the single and doubled truncation of the cluster operator (CCSD). The use of a relativistic Hamiltonian leads to a further increase in the computational cost of the coupled cluster calculation, and a relativistic CCSD^{23–25} method based on the two or four-component Hamiltonian is at least 32 times costlier than its nonrelativistic analog²⁶. The main reason behind elevation in the computational cost is the increase in the dimension due to four-component nature of the wavefunction comprising of large and small component spinors. One needs to uncontract the basis set to generate the necessary basis functiond for the small component using the kinetic balance condition^{26,27}. At the same time, one must store complex numbers for the Hamiltonian matrix elements, which also leads to increased computational cost.

To simplify this four-component formalism, two-component(quasi-relativistic) approaches²⁸⁻³⁰ have developed. This can be achieved by a unitary transformation, known as the Foldy-Wouthuysen (FW) transformation³¹. However, except for free electrons, performing this transformation can be challenging. An alternative approach, known as the Normalized Elimination of the Small Component (NESC) formalism³²⁻³⁵, is a computationally straightforward method that allows for exact solutions of the Dirac equation for fermionic systems. The primary cause behind this rise in computational cost in a two- or four-component calculation is spin-orbit coupling (SOC), which disrupts the spin-symmetry, significantly increasing the number of molecular orbital integrals (MO)³⁶. Although SOC effects are important in various scenarios, such as calculating energy differences in electronically degenerate states or simulating SOC-induced spin-forbidden transitions, they often have a relatively minor impact on many other properties³⁷. In such cases, a scalar-relativistic approach that omits SOC effects may be sufficient, as the SOC corrections are reflected in the second-order of the perturbative expansion for closed-shell systems. Dyll's method of decoupling scalar-relativistic (spin-free) and SOC (spin-dependent) effects has led to the development of spin-free four-component Dirac-Coulomb (SFDC) approaches³⁸. One can get a further simplification by using exact two component (X2C)^{29,39,40} approach within the spin-free framework. The X2C method comes in various flavors. In its simplest form, it diagonalizes the one-electron DC Hamiltonian matrix and uses the resulting two-component Hamiltonian matrix alongside the untransformed two-electron interactions. This method is referred to as X2C-1e⁴¹, and the corresponding spin-free version is called the SFX2C1e method. It has very little additional cost over nonrelativistic calculations. The SFX2C1e coupled cluster method has been implemented for ground state energy, gradient, harmonic frequencies⁴¹⁻⁴⁴, and excited states⁴⁵. In this work, we have extended the SFX2C1e coupled cluster method to second-order properties using the linear response framework.

2. Theory

2.1 Spin separation of relativistic Hamiltonian

In the presence of an external electric field or potential V , the Dirac equation for an electron can be represented in two-spinor form as^{46,47}

$$(V - E)\psi^L + c(\vec{\sigma} \cdot \vec{p})\psi^S = 0 \quad (1)$$

$$c(\vec{\sigma} \cdot \vec{p})\psi^L + (V - E - 2mc^2)\psi^S = 0 \quad (2)$$

Now in matrix formulation, the Dirac Hamiltonian should take the following form:

$$\mathbf{H}^D \Psi = \begin{pmatrix} V & c\vec{\sigma} \cdot \vec{p} \\ c\vec{\sigma} \cdot \vec{p} & V - 2c^2 \end{pmatrix} \begin{pmatrix} \psi^L \\ \psi^S \end{pmatrix} = 0 \quad (3)$$

where $\vec{\sigma}$ and \vec{p} represent Pauli's spin matrices and momentum vector, respectively and Ψ consists of large(ψ^L) and small components (ψ^S) of the wave function. The structure of \mathbf{H}^D the matrix reveals that the diagonal block is spin-independent, and the off-diagonal block is spin-dependent. So, one can separate the spin-free and spin-dependent parts by just constructing two terms from the partitioning of diagonal and off-diagonal blocks. Moreover,

the small component is also represented in terms of a pseudo-large component ϕ^L based on kinetic balance approximation as

$$|\psi^s\rangle = \frac{(\vec{\sigma} \cdot \vec{p})}{2c} |\phi^L\rangle \quad (4)$$

where both small and large components are expanded on the same basis as

$$|\psi_p^L\rangle = c_{\mu p}^L |\chi_\mu\rangle \quad (5)$$

$$|\psi_p^s\rangle = c_{\mu p}^s \frac{\vec{\sigma} \cdot \vec{p}}{2c} |\chi_\mu\rangle \quad (6)$$

Here, $|\chi_\mu\rangle$ is the atomic basis function and $c_{\mu p}^L$, $c_{\mu p}^s$ are the corresponding coefficients for large and small components, respectively. One can achieve the spin separation from the one-electron Dirac Hamiltonian by writing the modified Dirac Hamiltonian \mathbf{H}^M matrix as

$$\mathbf{H}^M \begin{pmatrix} \mathbf{C}^L \\ \mathbf{C}^s \end{pmatrix} = \begin{pmatrix} \mathbf{S} & \mathbf{0} \\ \mathbf{0} & \frac{1}{2c^2} \mathbf{T} \end{pmatrix} \begin{pmatrix} \mathbf{C}^L \\ \mathbf{C}^s \end{pmatrix} E \quad (7)$$

where,

$$\mathbf{H}^M = \begin{pmatrix} \mathbf{V} & \mathbf{T} \\ \mathbf{T} & \frac{1}{4c^2} \mathbf{W} \cdot \mathbf{T} \end{pmatrix} \quad (8)$$

where the \mathbf{S} , \mathbf{T} , \mathbf{V} and \mathbf{W} matrices elements are expressed as

$$[\mathbf{S}]_{\mu\nu} = \langle \chi_\mu | \chi_\nu \rangle \quad (9)$$

$$[\mathbf{T}]_{\mu\nu} = \left\langle \chi_\mu \left| \frac{\vec{p}^2}{2} \right| \chi_\nu \right\rangle \quad (10)$$

$$[\mathbf{V}]_{\mu\nu} = \langle \chi_\mu | \hat{V} | \chi_\nu \rangle \quad (11)$$

$$[\mathbf{W}]_{\mu\nu} = \langle \chi_\mu | (\vec{\sigma} \cdot \vec{p}) \hat{V} (\vec{\sigma} \cdot \vec{p}) | \chi_\nu \rangle \quad (12)$$

The modified Dirac Hamiltonian still consists of spin-dependent term in \mathbf{W} . Using Dirac identity we can separate the matrix of \mathbf{W} as

$$[\mathbf{W}]_{\mu\nu} = [\mathbf{W}]_{\mu\nu}^{SF} + [\mathbf{W}]_{\mu\nu}^{SD} \quad (13)$$

where,

$$[\mathbf{W}]_{\mu\nu}^{sf} = \langle \chi_\mu | (p \cdot V \cdot p) | \chi_\nu \rangle, \quad [\mathbf{W}]_{\mu\nu}^{sd} = \langle \chi_\mu | (i\sigma \cdot (\vec{p} \times V \vec{p})) | \chi_\nu \rangle \quad (14)$$

and now the modified wavefunction is

$$\psi^M = \begin{pmatrix} \psi^L \\ \phi^L \end{pmatrix} \quad (15)$$

So, the explicit definition of modified spin separated Dirac Hamiltonian is

$$\mathbf{H}^M = \begin{pmatrix} V & \hat{T} \\ \hat{T} & [W^{SF} - \hat{T}] / 4c^2 \end{pmatrix} + \begin{pmatrix} \mathbf{0} & \mathbf{0} \\ \mathbf{0} & W^{SD} / 4c^2 \end{pmatrix} = \mathbf{H}^{SF} + \mathbf{H}^{SD} \quad (16)$$

The solution of this modified Hamiltonian exactly matches the solution of the original one electron Dirac Hamiltonian, which signifies that the method used to separate out the spin-dependent and spin-independent part consists of no approximation⁴⁸.

The computational overhead due to the presence of the small component can be reduced by removing the small component from the wave function, which is done by Foldy-Wouthuysen (FW) unitary transformation.

$$\mathbf{U}^\dagger \mathbf{H}^M \mathbf{U} = \begin{pmatrix} \mathbf{H}_+^{FW} & 0 \\ 0 & \mathbf{H}_-^{FW} \end{pmatrix} \quad (17)$$

where,

$$\mathbf{U} = \begin{pmatrix} 1 & -\mathbf{X}^\dagger \\ \mathbf{X} & 1 \end{pmatrix} \begin{pmatrix} \mathbf{R} & 0 \\ 0 & \mathbf{R}' \end{pmatrix} = \mathbf{U}^X \mathbf{U}^R \quad (18)$$

In this transformation \mathbf{U}^X takes care of the block diagonalization and \mathbf{U}^R does the normalization on the modified Hamiltonian \mathbf{H}^M . The operator \mathbf{X} connects the small and large component coefficients, i.e.,

$$\mathbf{X} \mathbf{C}^L = \mathbf{C}^S \quad (19)$$

The coefficient of the two-component wave function after the transformation is related to the large component one by the operator $\hat{\mathbf{R}}$

$$\mathbf{C}_{FW}^{2C} = \frac{\mathbf{C}^L}{\hat{\mathbf{R}}} \quad (20)$$

Where \mathbf{R} is expressed as;

$$\hat{\mathbf{R}} = \mathbf{S}^{-\frac{1}{2}} \left(\mathbf{S}^{-\frac{1}{2}} \tilde{\mathbf{S}} \mathbf{S}^{-\frac{1}{2}} \right)^{-\frac{1}{2}} \mathbf{S}^{\frac{1}{2}} \quad (21)$$

And

$$\tilde{\mathbf{S}} = \mathbf{S} + \frac{1}{2c^2} \mathbf{X}^\dagger \mathbf{T} \mathbf{X} \quad (22)$$

The solution of \mathbf{H}_+^{FW} will correspond to the orbital energies, and through this FW transformation will result:

$$\mathbf{H}_+^{FW} \mathbf{C}_{FW}^{2C} = \mathbf{E}_+ \mathbf{S} \mathbf{C}_{FW}^{2C} \quad (23)$$

where \mathbf{E}_+ is the matrix corresponds to orbital energies and the \mathbf{H}_+^{FW} is expressed as

$$\mathbf{H}_+^{FW} = \hat{\mathbf{R}}^\dagger \mathbf{L}^{NESC} \hat{\mathbf{R}} \quad (24)$$

with

$$\mathbf{L}^{NESC} = \mathbf{V} + \mathbf{T} \mathbf{X} + \mathbf{X}^\dagger \mathbf{T} - \mathbf{X}^\dagger \mathbf{T} \mathbf{X} + \frac{1}{4c^2} \mathbf{X}^\dagger \mathbf{W} \mathbf{X} \quad (25)$$

The spin-free X2C one electron (SFX2C1e) method is obtained by taking the spin-free part \mathbf{H}^{SF} of the modified Hamiltonian \mathbf{H}^M and subsequently performing the FW transformation. One can simply use this two-component FW transformed spin-free modified Hamiltonian to

replace the one electron part of the nonrelativistic Hamiltonian and use the nonrelativistic two-electron integrals without any transformation. This will help to incorporate the scalar relativistic effect in SCF and electron-correlation calculations with negligible additional computational cost over a nonrelativistic calculation.

2.2 Linear response coupled cluster method

(a) Time-independent coupled cluster theory

In the coupled cluster method, the correlated ground state wavefunction can be written as an exponential ansatz over the reference (e.g., Hartree-Fock) wavefunction $|\Phi_0\rangle$ as

$$|\Psi_{CC}\rangle = e^{\hat{T}} |\Phi_0\rangle \quad (26)$$

Here, \hat{T} is the cluster operator, which has the form of

$$\hat{T} = \hat{T}_1 + \hat{T}_2 + \hat{T}_3 + \dots + \hat{T}_N = \sum_p^N \hat{T}_p \quad (27)$$

where

$$\hat{T}_p = \sum_{\substack{i>j>k>\dots \\ a>b>c>\dots}} t_{ijk\dots}^{abc\dots} \hat{a}_a^\dagger \hat{a}_b^\dagger \hat{a}_c^\dagger \dots \hat{a}_k \hat{a}_j \hat{a}_i \dots \quad (28)$$

One can write the cluster operator in a compact format as

$$\hat{T} = \sum_{\mu} t_{\mu} \hat{\tau}_{\mu} |\Phi_0\rangle \quad (29)$$

where $\hat{\tau}_{\mu}$ is used as a shorthand notation for the series of second quantized operators as,

$$\hat{\tau}_{\mu} = \hat{a}_a^\dagger \hat{a}_b^\dagger \hat{a}_c^\dagger \dots \hat{a}_k \hat{a}_j \hat{a}_i \dots \quad (30)$$

and t_{μ} is the corresponding amplitude.

One can use the generic notation $|\mu\rangle$ for excited determinant depending on the level of excitation

$$|\mu\rangle = |\Phi_i^a\rangle, |\Phi_{ij}^{ab}\rangle, |\Phi_{ijk\dots}^{abc\dots}\rangle \quad (31)$$

Where $|\Phi_i^a\rangle, |\Phi_{ij}^{ab}\rangle, |\Phi_{ijk\dots}^{abc\dots}\rangle$ are the singly, doubly and N -tuply excited state determinants respectively.

The coupled cluster energy and amplitude equations can be represented as

$$E_{CC} = \langle \Phi_0 | e^{-\hat{T}} \hat{H} e^{\hat{T}} | \Phi_0 \rangle \quad (32)$$

$$\langle \mu | e^{-\hat{T}} \hat{H} e^{\hat{T}} | \Phi_0 \rangle = 0 \quad (33)$$

Due to the non-Hermitian nature of coupled cluster similarity transformed Hamiltonian the left-hand wavefunction is not a complex conjugate of $|\Psi_{CC}\rangle$, rather it has a different form

$$\langle \tilde{\Psi}_{CC} | = \langle \Phi_0 | (1 + \hat{\Lambda}) e^{-\hat{T}} \quad (34)$$

where $\hat{\Lambda}$ is a linear de-excitation operator and defined as

$$\langle \Phi_0 | \hat{\Lambda} = \langle \Phi_0 | \sum_{\mu} \hat{\Lambda}_{\mu} = \langle \Phi_0 | \sum_{\mu} \lambda_{\mu} \hat{\tau}_{\mu}^{\dagger} = \sum_{\mu} \lambda_{\mu} \langle \mu | \quad (35)$$

The λ_{μ} are the corresponding amplitudes for de-excitations and

$$\langle \mu | = \langle \phi_0 | \hat{\tau}_{\mu}^{\dagger} \quad (36)$$

Similar to the t_{μ} amplitude equation described in eq. (34) the λ_{μ} amplitudes can also be obtained as:

$$\langle \Phi_0 | (1 + \hat{\Lambda}) [\bar{H}, \hat{\tau}_{\mu}] | \Phi_0 \rangle = 0 \quad (37)$$

(b) Time-dependent coupled cluster theory

The time evolution of coupled cluster wave-function under a time-dependent external perturbation can be denoted as

$$| \Psi_{cc}(t) \rangle = e^{\hat{T}(t)} | \Phi_0 \rangle e^{i\epsilon(t)} \quad (38)$$

and due to the non-Hermitian nature of CC Hamiltonian, it also leads to a distinct time dependent left-hand side analogue as

$$\langle \tilde{\Psi}_{cc}(t) | = \langle \Phi_0 | (1 + \hat{\Lambda}(t)) e^{-\hat{T}(t)} e^{-i\epsilon(t)} \quad (39)$$

Where $e^{i\epsilon(t)}$ implies a time dependent phase factor and $\hat{T}(t)$ is time dependent cluster operator with time-dependent amplitudes.

As the cluster operator is also time-dependent, they generate excited state determinants upon acting on the reference state with inherent time dependency in the cluster amplitudes $t_{\mu}(t)$ as,

$$\hat{T}(t) | \Phi_0 \rangle = \sum_{\mu} \hat{T}_{\mu}(t) | \Phi_0 \rangle = \sum_{\mu} t_{\mu}(t) \tau_{\mu} | \Phi_0 \rangle = \sum_{\mu} t_{\mu}(t) | \mu \rangle \quad (40)$$

Similarly, for the time-dependent de-excitation operator,

$$\langle \Phi_0 | \hat{\Lambda}(t) = \langle \Phi_0 | \sum_{\mu} \hat{\Lambda}_{\mu}(t) = \langle \Phi_0 | \sum_{\mu} \lambda_{\mu}(t) \tau_{\mu}^{\dagger} = \sum_{\mu} \lambda_{\mu}(t) \langle \mu | \quad (41)$$

It should be noted that the orbital response is not considered for the reference wave function. This time-dependent coupled cluster amplitudes $t_{\mu}(t)$ and $\lambda_{\mu}(t)$ are given by

$$\langle \mu | \bar{H} | \Phi_0 \rangle = i \frac{dt_{\mu}}{dt} \quad (42)$$

$$\langle \Phi_0 | (1 + \hat{\Lambda}) [\bar{H}, \tau_{\mu}] | \Phi_0 \rangle = -i \frac{d\lambda_{\mu}}{dt} \quad (43)$$

(c) Linear response function

The external response can be manifested by employing a time-dependent perturbation $\hat{V}^{(1)}(t)$ on the original time-independent Hamiltonian such as

$$\hat{H} = \hat{H}^{(0)} + \hat{V}^{(1)}(t) \quad (44)$$

This time-dependent operator $\hat{V}^{(1)}(t)$ can be converted into a frequency-dependent Hamiltonian $\hat{V}^{(1)}(\omega)$ using Fourier-Transformation⁴⁹ as

$$\hat{V}^{(1)}(t) = \int_{-\infty}^{\infty} d\omega \hat{V}^{(1)}(\omega) e^{-i\omega t} \quad (45)$$

and the linear response function for an exact state is given by

$$\langle\langle A, \hat{V}^{(1)}(\omega) \rangle\rangle = \sum_n \left(\frac{\langle \Phi_0 | A | \Psi_n \rangle \langle \Psi_n | \hat{V}^{(1)}(\omega) | \Phi_0 \rangle}{\omega - \omega_n} - \frac{\langle \Phi_0 | \hat{V}^{(1)}(\omega) | \Psi_n \rangle \langle \Psi_n | A | \Phi_0 \rangle}{\omega + \omega_n} \right) \quad (46)$$

Here Ψ_n is the solution of unperturbed Hamiltonian $\hat{H}^{(0)}$ and ω_n is the excitation energy corresponding to n^{th} state. Now the perturbed excitation and de-excitation cluster operators are expanded in terms of perturbation order as

$$\hat{T}(t) = \hat{T}^{(0)}(t) + \hat{T}^{(1)}(t) + \hat{T}^{(2)}(t) + \dots \quad (47)$$

$$\hat{\Lambda}(t) = \hat{\Lambda}^{(0)}(t) + \hat{\Lambda}^{(1)}(t) + \hat{\Lambda}^{(2)}(t) + \dots \quad (48)$$

The expression for the first order perturbed $t_\mu^{(1)}$ amplitude can be written as:

$$\omega t_\mu^{(1)}(\omega) = \langle \mu | \bar{V}^{(1)}(\omega) | \phi_0 \rangle + \langle \mu | [\bar{H}^{(0)}, \hat{T}^{(1)}(\omega)] | \phi_0 \rangle \quad (49)$$

Similarly, the perturbed amplitude equation for $\lambda_\mu^{(1)}$ have the following form

$$-\omega \lambda_\mu^{(1)}(\omega) = \langle \phi_0 | \hat{\Lambda}^{(1)}(\omega) [\bar{H}^{(0)}, \tau_\mu] | \phi_0 \rangle + \langle \phi_0 | (1 + \hat{\Lambda}^{(0)}) [\tilde{V}^{(1)}(\omega), \tau_\mu] | \phi_0 \rangle \quad (50)$$

where

$$\tilde{V}^{(1)}(\omega) = \bar{V}^{(1)}(\omega) + [\bar{H}^{(0)}, \hat{T}^{(1)}(\omega)] \quad (51)$$

The time-dependent expectation value of an operator A can be written as

$$\langle \hat{A}(t) \rangle = \langle \phi_0 | (1 + \hat{\Lambda}(t)) \bar{A} | \phi_0 \rangle \quad (52)$$

Consequently, the coupled cluster linear response function may be represented as,

$$\langle\langle \hat{A}; \hat{V}^{(1)}(\omega) \rangle\rangle = \langle \phi_0 | [(1 + \hat{\Lambda}^{(0)}) [\bar{A}^{(0)}, \hat{T}^{(1)}(\omega)] + \hat{\Lambda}^{(1)}(\omega) \bar{A}^{(0)}] | \phi_0 \rangle \quad (53)$$

It can be seen that the linear response function, as described above, is asymmetric in nature as it involves both perturbed \hat{T} and $\hat{\Lambda}$ operator. One can also express the linear response function in its symmetric form by writing it only in terms of perturbed $\hat{T}^{(1)}(\omega)$ operator, which will consist quadratic terms of $\hat{T}^{(1)}(\omega)$.

$$\begin{aligned} \langle\langle \hat{A}; \hat{V}^{(1)}(\omega) \rangle\rangle &= \langle \phi_0 | [(1 + \hat{\Lambda}^{(0)}) [\bar{A}^{(0)}, \hat{T}_{\hat{V}^{(1)}}^{(1)}(\omega)] | \phi_0 \rangle + \langle \phi_0 | [\hat{V}^{(1)}(\omega), \hat{T}_{\hat{A}}^{(1)}(-\omega)] | \phi_0 \rangle \\ &\quad + \langle \phi_0 | [[\bar{H}^{(0)}, \hat{T}_{\hat{V}^{(1)}}^{(1)}(\omega)], \hat{T}_{\hat{A}}^{(1)}(-\omega)] | \phi_0 \rangle \end{aligned} \quad (54)$$

In this manuscript, we have used the asymmetric formalism as described in eq (53) for the polarizability calculation. The dipole polarizability tensor within the linear response function can be represented as

$$\langle\langle \boldsymbol{\mu}; \boldsymbol{\mu} \rangle\rangle = \left\langle \phi_0 \left[\left(1 + \hat{\Lambda}^{(0)} \right) \left[\bar{\boldsymbol{\mu}}, \hat{T}^{(1)}(\omega) \right] + \hat{\Lambda}^{(1)}(\omega) \bar{\boldsymbol{\mu}} \right] \phi_0 \right\rangle \quad (55)$$

where $\bar{\boldsymbol{\mu}}$ is the similarity transformed dipole moment. Subsequent symmetrisation and trace of the polarizability tensor finally gives the total polarizability

$$\alpha(\omega) = \frac{1}{3} \text{Tr} \left[\langle\langle \boldsymbol{\mu}; \boldsymbol{\mu} \rangle\rangle \right] \quad (56)$$

(d) Density Fitting Approximation

To further reduce the storage and computational overhead larger, we have employed density fitting approximation where four centre-two electron integrals are replaced by three centre two-electron integrals which reduces the computational cost^{50,51} significantly. The four-centered two-electron integrals $(pq | rs)$ in case of real orbitals can be defined as,⁵²

$$(pq | rs) = \int dr_1 \int dr_2 \phi_p(r_1) \phi_q(r_1) \frac{1}{r_{12}} \phi_r(r_2) \phi_s(r_2) \quad (57)$$

One can rewrite the expression for two-electron integral as,

$$(pq | rs) = \int dr_1 \int dr_2 \boldsymbol{\rho}_{pq}(r_1) \frac{1}{r_{12}} \boldsymbol{\rho}_{rs}(r_2) \quad (58)$$

Where, $\boldsymbol{\rho}_{xy} = \phi_x(r) \phi_y(r)$. An auxiliary basis can be used to fit $\boldsymbol{\rho}_{xy}$ as,

$$\bar{\boldsymbol{\rho}}_{xy}(r) = \sum_P^{N_{aux}} \mathbf{d}_P^{xy} \chi_P(r) \quad (59)$$

Here, \mathbf{d}_P^{xy} and χ_P are the fitting coefficients of the auxiliary basis and auxiliary basis functions respectively. one can express \mathbf{d}_P^{xy} as,

$$\mathbf{d}_P^{xy} = \sum_Q (xy | Q) [\mathbf{X}^{-1}]_{QP} \quad (60)$$

where, $(xy | Q)$ is the three-centered two-electron integral, defined as,

$$(xy | Q) = \int dr_1 \int dr_2 \phi_x(r_1) \phi_y(r_1) \frac{1}{r_{12}} \chi_Q(r_2) \quad (61)$$

and

$$\mathbf{X}_{QP} = \int dr_1 \int dr_2 \chi_Q(r_1) \frac{1}{r_{12}} \chi_P(r_2) \quad (62)$$

The four-centered two-electron integral $(pq | rs)$ can be constructed from the three-centered two-electron integrals which are fitted by an auxiliary basis⁵³⁻⁵⁵,

$$\begin{aligned}
(pq | rs) &= \int dr_1 \int dr_2 \sum_Q \mathbf{d}_Q^{pq} \chi_Q(r_1) \frac{1}{r_{12}} \chi_r(r_2) \chi_s(r_2) \\
&= \sum_Q \mathbf{d}_Q^{pq} (Q | rs) \\
&= \sum_{PQ} (pq | P) [\mathbf{X}^{-1}]_{PQ} (Q | rs) \\
&= \sum_{PQR} (pq | P) [\mathbf{X}^{-\frac{1}{2}}]_{PQ} [\mathbf{X}^{-\frac{1}{2}}]_{QR} (R | rs) \\
&= \sum_Q \left\{ \sum_P (pq | P) [\mathbf{X}^{-\frac{1}{2}}]_{PQ} \right\} \left\{ \sum_R [\mathbf{X}^{-\frac{1}{2}}]_{QR} (R | rs) \right\} \\
&= \sum_Q \mathbf{J}_{pq}^Q \mathbf{J}_{rs}^Q
\end{aligned} \tag{63}$$

where

$$\mathbf{J}_{pq}^Q = \sum_P (pq | P) [\mathbf{X}^{-\frac{1}{2}}]_{PQ} \tag{64}$$

The factorized linear response coupled cluster equations in the term three centered two electron intermediates are presented in the supporting information. The integrals up to two external indices are constructed once and stored in the disk. The integrals with three and four external indices are never constructed explicitly, and the terms involving these integrals are always constructed on the fly from three-centered two-electron integrals. It should be noted that the density fitting approximation can only reduce the formal scaling Coulomb kind of terms unless special techniques are used^{56–59}. However, the reduction in disk i/o still leads to significant speed up even for exchange terms.

A pictorial representation of the steps involved in SFX2C1e-LRCCSD method have been shown in Figure 1.

3. Computational Details

All the SFX2C1e-LRCCSD polarizability calculations based on coupled cluster linear response framework are carried out using our in-house quantum chemistry software package BAGH⁶⁰. The converged SFX2C1e Hartree-Fock coefficient and one electron and three centred two-electron integrals were taken from PYSCF v2.1. The auxiliary functions were generated automatically based on the orbital basis set in PYSCF. The frozen core approximation was used all the test cases. Experimental geometry has been used for all the molecules and the corresponding cartesian coordinates are provided in the supporting information.

4. Results and Discussion

4.1 Polarizability of atoms:

The basis set plays a vital role in determining the accuracy of the calculated polarizability values. To understand the effect of the basis set on the SFX2C1e-LRCCSD polarizability values, we have investigated the basis set dependence on the dynamic polarizability values on Kr atom. For this purpose, we have used dyall.aenz (n=2,3,4) basis set. It is well known that accurate polarizability calculations require the inclusion of sufficient diffuse functions in the basis set⁶¹. To see the effect of diffuse functions on the calculation, we have augmented the basis set with single, double, triple, and quadruple sets of diffuse functions. These augmented basis sets are generated using DIRAC-19^{62,63} software package.

From Table 1 it can be observed that the absence of diffuse functions leads to considerable error. Specifically, the deviation in SFX2C1e-LRCCSD results in the dyall.ae2z basis set amounts to 9.737 atomic units when compared to the experimental values. The error reduces to 4.966 a.u., when dyall.ae3z basis set is used. The error does not converge even when the dyall.ae4z basis set is used. But even a single augmentation at dyall.ae2z level reduces the error to 0.404 a.u. The results generally converge with the triple augmentation of the basis set at double and triple zeta levels, whereas single augmentation is sufficient at quadruple zeta levels. It can be seen that augmentation of the basis set for a particular cardinal number leads to an increase in the polarizability values. The triply augmented triple zeta results show better agreement with the experiment than the corresponding quadrupole zeta basis set, presumably due to fortuitous error cancelation. Tables S1 and S2 present the polarizability values of group 2 and group 18 elements in t-aug-dyall.ae3z and s-aug-dyall.ae4z basis set. It can be seen that the results in these two basis sets are generally in close agreement with each other, similar to that observed for the Kr atom. The results are also in good agreement with the available experimental results. Therefore, the s-aug-Dyall.ae4z can be taken as an optimal basis set for the calculation. To understand the magnitude of the error caused by density fitting approximation, we have plotted the dynamic polarizability value of Zn, Cd, and Hg for the frequency range 0.0-0.3 a.u. with and without density fitting in Figure 2. It can be seen that the use of density fitting approximation leads to very negligible error in the SFX2C1e-LRCCSD calculations, and the plots with and without density fitting are almost indistinguishable from each other. Therefore, the rest of the calculations in the manuscript are performed employing density fitting approximation.

Table 2 describes the effect of relativity and correlation on static and dynamic polarizability. s-aug-dyall.v2z basis set has been used for the calculations. The Hartree-Fock polarizabilities were calculated using the sum over state (SOS)⁶⁴ formula using TDHF⁶⁵⁻⁶⁸ energy and wave function. It can be seen that the effect of correlation and relativity both lead to the reduction of the polarizability values. The relativistic effect has a small impact on the static polarizability of Zn and the error in NR-LR-CCSD result is 6 percent with respect to its SFX2C1e version. The error increases as we go down the group, and the neglect of the relativistic effect can lead to errors as high as 19 and 69 percent for Cd and Hg, respectively. Even in the case of Zn, the impact of relativity on dynamic polarizability is considerable, with a notable 12 percent

disparity observed between relativistic and nonrelativistic LR-CCSD at a frequency of 0.14014 atomic units.

Similarly, the electron correlation shows a larger effect as the frequency increases. The inclusion of electron correlation leads to 38 percent decrease in the dynamic polarizability (0.14014) with respect to SFX2C1e Hartree-Fock for Zn. It can be seen that effect correlation is more prominent for the nonrelativistic case than in the case of the relativistic CCSD method. The effect of correlation is most prominent for dynamic polarizability of Hg at the frequency 0.1401a.u., where one can observe of reduction is 77 on going from nonrelativistic Hartree-Fock to nonrelativistic LR-CCSD method. For the same frequency, the corresponding reduction is 35 percent in the case of relativistic calculation, which is almost half of the nonrelativistic one.

Gomes and co-workers¹¹ have performed a detailed analysis of the pole structure of the dynamic polarizability tensor for Zn, Cd, and Hg in their X2C-LRCCSD study. In this work, we have extended the analysis to nonrelativistic and SFX2C1e-LRCCSD methods. In Figure 3, we have plotted the calculations done at three different levels of theories: nonrelativistic LR-CCSD, SFX2C1e-LRCCSD, and exact two-component LR-CCSD (X2C-LRCCSD). The X2C-LRCC results were taken from reference²⁰. For Zn and Cd, the poles correspond to two $ns \rightarrow np$ transitions (A and B denote spin-forbidden $^1S_0 \rightarrow ^3P_1^0$ and spin-allowed $^1S_0 \rightarrow ^1P_0$ transitions, respectively) and two $ns \rightarrow (n+2)p$ transitions (C and D, similarly spin-forbidden and spin-allowed transitions, respectively). Only the first two poles corresponding to $ns \rightarrow np$ transition is present for Hg in the frequency range considered by Gomes and co-workers. It can be seen that the frequency-dependent polarizability spectrum of Zn, Cd, and Hg obtained from the SFX2C1e variant closely resembles the trend calculated at the full X2C-LRCCSD level. The polarizability spectrum generated from the SFX2C1e-LRCCSD matches significantly with the X2C-LRCCSD results for the entire frequency range except regions A and C. It proves that second-order response properties can be accurately simulated with only the inclusion of a spin-independent core Hamiltonian containing the scalar relativistic effects. For closed shell molecule, the spin-free Hamiltonian contributes at first order of perturbation to the relativistic Hamiltonian, while the spin-dependent part of the Hamiltonian comes up as higher orders of perturbative correction for closed-shell molecules. It should be noted that the deviation between relativistic and nonrelativistic results is more prominent at higher frequencies, which is most evident for Hg. Although the SFX2C1e-LRCCSD and X2C-LRCCSD give excellent agreement for most of the frequency ranges, the former misses the poles corresponding to spin-forbidden excited states present in the X2C-LRCCSD. For instance, when considering the element Zn, the peaks obtained at frequencies 0.140 a.u. (A) and 0.27 a.u. (C) in X2C-LRCCSD calculations are not observed in SFX2C1e and nonrelativistic results. These poles correspond to the spin-forbidden $^1S_0 \rightarrow ^3P_1$ transitions arising due to the spin-orbit coupling (SOC), which cannot be captured by the SFX2C1e method where the spin-dependent terms are absent. The SFX2C1e-LRCCSD method, however, accurately reproduces the poles at ~0.2089 a.u. (B) and 2828 a.u. (D) which arise due to spin-allowed $^1S_0 \rightarrow ^1P_0$ transitions. A similar pattern is observed for Cd and Hg., where the peaks due to spin-forbidden transitions cannot be captured by the SFX2C1e model

As we have seen, the basis set plays a crucial role in determining the accuracy of the calculated polarizabilities, especially when one is interested in comparing with experimental results. Table 3 presents the static and dynamic polarizabilities for Zn, Cd, and Hg in SFX2C1e-LR-CCSD/s-aug-dyall.ae4z level of theory, along with its experimental values. We have also included the X2C-LRCCSD results by Gomes and co-workers²⁰ in our comparison. The static and polarizabilities determined using the SFX2C1e-LRCCSD method show good agreement with the experimental values. The SFX2C1e-LRCCSD static polarizability values overestimate the experimental results by 0.54 a.u. and 1.12 a.u. for Zn and Hg. On the other hand, the static polarizability value for Cd is underestimated by 0.69 a.u. This slight deviation may be attributed to the contribution from spin-orbital coupling and higher-order correlation corrections missing in the present implementation. The nonrelativistic static polarizability value for Hg shows an error of 72.6% with respect to the experiment. This demonstrates the importance of the inclusion of the relativistic effect for polarizability calculations of heavy elements. The deviation between the experimental values and the SFX2C1e-LRCCSD static polarizability values are smaller than those reported by Gomes and co-workers²⁰ for the X2C-LRCCSD method. This could be due to the use of a smaller s-aug-dyall.v2z basis set in their calculations. Table 3 also presents the dynamic polarizability values at three different frequencies. The SFX2C1e-LRCCSD method for Zn shows 1.65%, 1.83%, and 1.90% of error with respect to experiment for dynamic polarizabilities at frequencies 0.07198 a.u., 0.08383 a.u., and 0.14014 a.u.. Higher errors are observed for Cd and Hg, which is presumably due to the higher magnitude of spin-orbital coupling. Conversely, the nonrelativistic LRCCSD method fails to accurately reproduce the dynamic polarizabilities, even in a qualitative sense. For Zn, the nonrelativistic dynamic polarizability value at a frequency of 0.14014 a.u. exhibits an error of 15.36% relative to the experiment. The error can reach as high as 188.1% for Hg at the same frequency.

4.3 Polarizability of molecules:

Molecular polarizability can be different from atomic polarizability as the molecule lacks the spherical symmetry of atoms. One can calculate the mean polarizability of a molecule which

is defined as

$$\bar{\alpha}(\omega) = \frac{\alpha_{xx}(\omega) + \alpha_{yy}(\omega) + \alpha_{zz}(\omega)}{3} \quad (65)$$

and the anisotropic polarizability can be described as

$$\gamma(\omega) = \alpha_{zz}(\omega) - \frac{1}{2}(\alpha_{xx}(\omega) + \alpha_{yy}(\omega)) \quad (66)$$

In Table 4, we have presented the static polarizabilities of AuH. Since no experimental data for the static polarizability is available for AuH, we have compared the SFX2C1e-LR-CCSD values with the previously reported 4c-DFT linear response results by Salek *et al*¹⁶. The double and triple zeta quality basis set chosen in the present work is slightly different from the 4c-DFT calculations. In the 4c-DFT calculation, the used basis sets were of dimensions 22s19p12d9f and 29s24p15d11f. On the other hand, we employed dyall.ae2z and dyall.ae3z basis sets with

dimensions *24s19p12d9f1g* and *30s24p15d11f5g1h*, respectively. For hydrogen *Salek et al* have used Dunning’s de-contracted aug-cc-pVXZ (X=D, T) basis set, but we used the same in its contracted form. The mean, parallel, and perpendicular polarizability components calculated at SFX2C1e-LRCCSD level reasonably agree with the DFT values for all three functionals. The absolute numerical values differ from functional to functional, but the increase in the polarizability value in SFX2C1e-LRCCSD method with the increase of basis set size is also a common trend observable for all the functionals.

In Table 5, we have presented static polarizabilities of hydrogen halides (HX, where X=F, Cl, Br, I), iodine dimer, and molecules made of alkali metals, i.e. NaLi and CsK. Gomes and co-workers used the same set of molecules to benchmark their X2C-LRCCSD implementation. To demonstrate the performance of the SFX2C1e-LRCCSD method, we have compared our results with the X2C-LRCCSD variant. To separate out the relativistic effect from the basis set effect, we have used the same basis set that Gomes and co-workers²⁰ used for the isotropic static polarizability calculation of diatomic molecules, i.e. uncontracted aug-cc-pVDZ for lighter elements (H, F, Cl, Br) and s-aug-dyall.v2z basis set for heavier elements (I, Cs). The SFX2C1e-LRCCSD method shows a difference of 0.08 a.u., 0.02 a.u., 0.08 a.u for HF, HCl and HBr, respectively, with respect to the X2C-LRCCSD method. A slightly higher deviation from X2C results was observed for HI, ICl, and I₂, ranging from 0.3 a.u. to 0.5 a.u. between two methods. This is presumably due to the effect of spin-orbit coupling present in X2C Hamiltonian. In case of metal dimers NaK and CsK show a much higher magnitude of deviation, where SFX2C1e-LRCCSD underestimates the static polarizability by 4 a.u. with respect to the X2C-LRCCSD result. It is not appropriate to compare the results in a double zeta quality basis set with the experimental results. The use of a larger basis set may be extremely expensive in X2C or four-component Dirac-Coulomb Hamiltonian. However, the density fitting-based implementation of SFX2C1e-LRCCSD allows one to use a larger basis set in the calculations.

Figure 4 presents the error in static polarizability values with respect to the experiment. It can be seen that the SFX2C1e-LRCCSD method shows a very similar error with respect to the experiment as that of the X2C-LRCCSD method in the double zeta basis set. The agreement of SFX2C1e-LRCCSD results with the experiment improves when going to the d-aug-Dyall.v4z basis set for all molecules except ICl and NaLi. Figure 3 presents the percentage error with respect to the experiment in SFX2C1e and X2C-LRCCSD. It shows that the basis set has larger effects than the spin-orbit coupling for most of the molecule, at least for the static polarizabilities. The static polarizability values for the ICl and NaLi in the SFX2C1e-LRCCSD method in a double zeta quality basis set are very similar to that of the X2C method. The reason for the increased discrepancy with respect to the experiment with the increase in the basis set dimension is not very clear at this moment.

Experimental dynamic polarizability of iodine dimer were available from the work of Maroulis *et al.* They measured the polarizability of I₂ at three different frequencies: 0.07198 a.u., 0.07669 a.u., and 0.140114 a.u. Gomes and co-workers²⁰ have reported X2C-LRCCSD dynamic polarizability at the same frequency using s-aug-dyall.v2z basis set. We have calculated SFX2C1e-LRCCSD dynamic polarizability at the same frequency using the same

basis set. From Table 6, it can be seen that the experimental polarizability of I₂ increases with the frequency, and it is gratifying to note that a similar trend is also observed for the SFX2C1e-LRCCSD results. The X2C-LRCCSD dynamic polarizabilities increase from frequency 0.07198 a.u. to 0.07669 a.u. but decreases from 0.07669 a.u. to 0.14014 a.u. Table 6 also presents the relativistic polarizabilities at HF and DFT levels based on the B3LYP functional. For all three levels of theory, the parallel component $\alpha_{xx}(\omega)$ does not vary significantly with the frequency and it is also observed that the effect of correlation is not that prominent for $\alpha_{xx}(\omega)$, whereas $\alpha_{zz}(\omega)$ is significantly sensitive to the electronic correlation effect and the level of theory. One can see that the parallel component shows a negative value at 0.07198 a.u. and 0.07669 a.u. for HF and DFT, respectively, signifying that near these two frequencies, they have poles in the polarizability spectrum, whereas no negative polarizability is observed either for SFX2C1e-LRCCSD or X2C-LRCCSD level of calculation.

The presence of density fitting allows one to apply the SFX2C1e-LRCCSD method beyond diatomic molecules. We have selected three molecules, namely Uranium Hexafluoride (UF₆), Osmium Tetraoxide (OsO₄), and Mercury Chloride (HgCl₂), for which experimental static polarizability values are available. Previous theoretical estimations of static polarizability for these three molecules are done by Cremer and co-workers⁴⁴ using analytical second derivatives of energy based on the Normalized Elimination of Small Component (NESC) framework. In Table 7, we have included the computed static polarizability values obtained using the SFX2C1e-LRCCSD approach, as well as the DFT and MP2 values as reported by Cremer and co-workers⁴⁴. Additionally, the table includes experimental values for comparison. We have used SARC-DKH (U, Os and Hg) and def2-QZVPP (F, O and Cl) basis set, which was also used by Cremer and co-workers⁴⁴. The perpendicular and parallel components of UF₆ and OsO₄ calculated at SFX2C1e-LRCCSD level are exactly the same as expected from symmetric octahedral and tetrahedral symmetry of the molecular structures, respectively. On the other hand, HgCl₂ has different values of parallel and perpendicular components due to its linear structure. An intriguing observation from Table 7 pertains to the discrepancy between the experimental values. Among the three molecules, OsO₄ shows a good agreement with the experimental value, but UF₆ and HgCl₂ results largely deviate from the available experimental values with an underestimation of 30.63 a.u. and 23.4 a.u. respectively in SFX2C1e-LRCCSD method. A similar disagreement with the experiment is also observed for the previously reported DFT and MP2 results. It should be noted that in the experimental numbers provided here contain both electronic as well as vibrational contributions to the total mean polarizability of these molecules. In the case of OsO₄, the electronic contribution of the total experimental mean polarizability⁶⁹ is 51.0 ± 1.0 a.u. and the SFX2C1e-LRCCSD results are in excellent agreement with the experiment with an overestimation of 0.45 a.u. for electronic polarizability. Meanwhile, MP2 and DFT results deviated by 3.54 and 5.5 a.u., respectively. The estimated electronic contribution⁶⁹ to the total polarizability for UF₆ is 66.6 ± 2.0 a.u. It can be seen that the SFX2C1e-LRCCSD method shows a large deviation of 14.21 a.u. for UF₆. Similarly, when considering DFT calculations, a deviation of 15.25 a.u. is observed. The deviation is 12.41 a.u. at the MP2 level. This deviation from the experiment in case of UF₆ for all the level of theories indicate a need for reconsideration and further refinement of the experiment for the static polarizability values of UF₆. The experimental mean polarizability of HgCl₂ is 78.2 a.u.

However, the estimates for the individual electronic and vibrational contributions to the polarizability of HgCl_2 vary significantly, with the electronic contribution ranging from 57 a.u. to 75 a.u., and the vibrational contribution ranging from 3 a.u. to 21 a.u. The SFX2C1e-LRCCSD method agrees well with the lower range of the electronic contribution.

5. Conclusions

We present the theory, implementation, and benchmarking of spin-Free exact two-component linear response coupled cluster method for static and dynamic polarizability. The SFX2C1e-LRCCSD method can make a balanced inclusion of relativistic and electron correlation effects. Density fitting approximation has been used to reduce the computational cost of the calculations, allowing one to calculate the static and dynamic polarizability at The SFX2C1e-LRCCSD level of theory beyond diatomic molecules. The SFX2C1e-LRCCSD method gives excellent agreement with the X2C-LRCCSD result at a much smaller computational cost. Our calculation shows that using a large basis set is as important as including electron correlation and relativistic effect for accurate simulation of polarizabilities of atoms and molecules containing heavy. The dynamic polarizabilities are more sensitive to the electron correlation and relativistic effect, and their importance increases with the increase in frequency. The SFX2C1e-LRCCSD method accurately reproduces the pole structure in the dynamic polarizability spectrum corresponding to spin-allowed transition but misses the poles corresponding to the spin-forbidden transformation. A potential solution to address the computational cost and/or absence of spin-forbidden poles in the polarizability spectrum, which currently affects the existing relativistic LR-CCSD implementations, is to develop a lower scaling LRCCSD method using a four-component relativistic Hamiltonian. Work is in progress towards that direction.

Supporting Information

The static polarizability of alkaline-earth metals (Be, Mg, Ca, Sr, Ba, Ra) and inert elements (He, Ne, Ar, Kr, Xe, Rn), and the used cartesian coordinates of HF, HCl, HBr, HI, I₂, ICl, Na-Li, Cs-K, HgCl₂, OsO₄ and UF₆ are presented in the supporting information.

7. References

- ¹ H.J. Monkhorst, "Calculation of properties with the coupled-cluster method," *International Journal of Quantum Chemistry* **12**(S11), 421–432 (1977).
- ² B. Datta, P. Sen, and D. Mukherjee, "Coupled-Cluster Based Linear Response Approach to Property Calculations: Dynamic Polarizability and Its Static Limit," *J. Phys. Chem.* **99**(17), 6441–6451 (1995).
- ³ H. Koch, H.J.Aa. Jensen, P. Jørgensen, and T. Helgaker, "Excitation energies from the coupled cluster singles and doubles linear response function (CCSDLR). Applications to Be, CH₄, CO, and H₂O," *The Journal of Chemical Physics* **93**(5), 3345–3350 (1990).
- ⁴ H. Sekino, and R.J. Bartlett, "A linear response, coupled-cluster theory for excitation energy," *International Journal of Quantum Chemistry* **26**(S18), 255–265 (1984).
- ⁵ M.E. Casida, "Time-Dependent Density Functional Response Theory for Molecules," in *Recent Advances in Density Functional Methods*, (WORLD SCIENTIFIC, 1995), pp. 155–192.
- ⁶ O. Christiansen, H. Koch, and P. Jørgensen, "The second-order approximate coupled cluster singles and doubles model CC2," *Chemical Physics Letters* **243**(5), 409–418 (1995).
- ⁷ O. Christiansen, P. Jørgensen, and C. Hättig, "Response functions from Fourier component variational perturbation theory applied to a time-averaged quasienergy," *International Journal of Quantum Chemistry* **68**(1), 1–52 (1998).
- ⁸ O. Christiansen, J. Gauss, and J.F. Stanton, "Frequency-dependent polarizabilities and first hyperpolarizabilities of CO and H₂O from coupled cluster calculations," *Chemical Physics Letters* **305**(1), 147–155 (1999).
- ⁹ K. Hald, F. Pawłowski, P. Jørgensen, and C. Hättig, "Calculation of frequency-dependent polarizabilities using the approximate coupled-cluster triples model CC3," *The Journal of Chemical Physics* **118**(3), 1292–1300 (2003).
- ¹⁰ R. Kobayashi, H. Koch, and P. Jørgensen, "Calculation of frequency-dependent polarizabilities using coupled-cluster response theory," *Chemical Physics Letters* **219**(1), 30–35 (1994).
- ¹¹ E.S. Nielsen, P. Jørgensen, and J. Oddershede, "Transition moments and dynamic polarizabilities in a second order polarization propagator approach," *The Journal of Chemical Physics* **73**(12), 6238–6246 (1980).
- ¹² J.R. Hammond, W.A. de Jong, and K. Kowalski, "Coupled-cluster dynamic polarizabilities including triple excitations," *The Journal of Chemical Physics* **128**(22), 224102 (2008).
- ¹³ B. Swirles, "The relativistic self-consistent field," *Proceedings of the Royal Society of London. Series A-Mathematical and Physical Sciences* **152**(877), 625–649 (1935).

- ¹⁴ T. Saue, and H.J.A. Jensen, "Linear response at the 4-component relativistic level: Application to the frequency-dependent dipole polarizabilities of the coinage metal dimers," *Journal of Chemical Physics* **118**(2), 522–536 (2003).
- ¹⁵ J.R. Hammond, N. Govind, K. Kowalski, J. Autschbach, and S.S. Xantheas, "Accurate dipole polarizabilities for water clusters $n=2-12$ at the coupled-cluster level of theory and benchmarking of various density functionals," *The Journal of Chemical Physics* **131**(21), 214103 (2009).
- ¹⁶ P. Salek, T. Helgaker, and T. Saue, "Linear response at the 4-component relativistic density-functional level: Application to the frequency-dependent dipole polarizability of Hg, AuH and PtH₂," *Chemical Physics* **311**(1-2 SPEC.ISS.), 187–201 (2005).
- ¹⁷ K. Burke, "Perspective on density functional theory," *The Journal of Chemical Physics* **136**(15), 150901 (2012).
- ¹⁸ D. Hait, and M. Head-Gordon, "How accurate are static polarizability predictions from density functional theory? An assessment over 132 species at equilibrium geometry," *Physical Chemistry Chemical Physics* **20**(30), 19800–19810 (2018).
- ¹⁹ I. Shavitt, and R.J. Bartlett, *Many-Body Methods in Chemistry and Physics: MBPT and Coupled-Cluster Theory* (Cambridge University Press, Cambridge, 2009).
- ²⁰ X. Yuan, L. Halbert, J.V. Pototschnig, A. Papadopoulos, S. Coriani, L. Visscher, and A.S. Pereira Gomes, "Formulation and Implementation of Frequency-Dependent Linear Response Properties with Relativistic Coupled Cluster Theory for GPU-Accelerated Computer Architectures," *J. Chem. Theory Comput.* **20**(2), 677–694 (2024).
- ²¹ J. Čížek, "On the Correlation Problem in Atomic and Molecular Systems. Calculation of Wavefunction Components in Ursell-Type Expansion Using Quantum-Field Theoretical Methods," *The Journal of Chemical Physics* **45**(11), 4256–4266 (1966).
- ²² J. Paldus, J. Čížek, and I. Shavitt, "Correlation Problems in Atomic and Molecular Systems. IV. Extended Coupled-Pair Many-Electron Theory and Its Application to the BH₃ Molecule," *Phys. Rev. A* **5**(1), 50–67 (1972).
- ²³ E. Lindroth, "Numerical solution of the relativistic pair equation," *Phys. Rev. A* **37**(2), 316–328 (1988).
- ²⁴ L. Visscher, T.J. Lee, and K.G. Dyall, "Formulation and implementation of a relativistic unrestricted coupled-cluster method including noniterative connected triples," *The Journal of Chemical Physics* **105**(19), 8769–8776 (1996).
- ²⁵ L. Visscher, E. Eliav, and U. Kaldor, "Formulation and implementation of the relativistic Fock-space coupled cluster method for molecules," *The Journal of Chemical Physics* **115**(21), 9720–9726 (2001).

- ²⁶ R.E. Stanton, and S. Havriliak, "Kinetic balance: A partial solution to the problem of variational safety in Dirac calculations," *The Journal of Chemical Physics* **81**(4), 1910–1918 (1984).
- ²⁷ K.G. Dyall, and K. Fægri, "Kinetic balance and variational bounds failure in the solution of the Dirac equation in a finite Gaussian basis set," *Chemical Physics Letters* **174**(1), 25–32 (1990).
- ²⁸ W. Kutzelnigg, and W. Liu, "Quasirelativistic theory I. Theory in terms of a quasi-relativistic operator," *Molecular Physics* **104**(13–14), 2225–2240 (2006).
- ²⁹ W. Kutzelnigg, and W. Liu, "Quasirelativistic theory equivalent to fully relativistic theory," *The Journal of Chemical Physics* **123**(24), 241102 (2005).
- ³⁰ M. Iliaš, and T. Saue, "An infinite-order two-component relativistic Hamiltonian by a simple one-step transformation," *The Journal of Chemical Physics* **126**(6), 064102 (2007).
- ³¹ L.L. Foldy, and S.A. Wouthuysen, "On the Dirac Theory of Spin 1/2 Particles and Its Non-Relativistic Limit," *Phys. Rev.* **78**(1), 29–36 (1950).
- ³² K.G. Dyall, "Interfacing relativistic and nonrelativistic methods. I. Normalized elimination of the small component in the modified Dirac equation," *The Journal of Chemical Physics* **106**(23), 9618–9626 (1997).
- ³³ K.G. Dyall, "Interfacing relativistic and nonrelativistic methods. II. Investigation of a low-order approximation," *The Journal of Chemical Physics* **109**(11), 4201–4208 (1998).
- ³⁴ K.G. Dyall, and T. Enevoldsen, "Interfacing relativistic and nonrelativistic methods. III. Atomic 4-spinor expansions and integral approximations," *The Journal of Chemical Physics* **111**(22), 10000–10007 (1999).
- ³⁵ K.G. Dyall, "Interfacing relativistic and nonrelativistic methods. IV. One- and two-electron scalar approximations," *Journal of Chemical Physics* **115**(20), 9136–9143 (2001).
- ³⁶ L. Cheng, and J. Gauss, "Analytical evaluation of first-order electrical properties based on the spin-free Dirac-Coulomb Hamiltonian," *The Journal of Chemical Physics* **134**(24), 244112 (2011).
- ³⁷ T. Kirsch, F. Engel, and J. Gauss, "Analytic evaluation of first-order properties within the mean-field variant of spin-free exact two-component theory," *The Journal of Chemical Physics* **150**(20), 204115 (2019).
- ³⁸ K.G. Dyall, "An exact separation of the spin-free and spin-dependent terms of the Dirac-Coulomb-Breit Hamiltonian," *The Journal of Chemical Physics* **100**(3), 2118–2127 (1994).
- ³⁹ W. Kutzelnigg, "Relativistic one-electron Hamiltonians 'for electrons only' and the variational treatment of the Dirac equation," *Chemical Physics* **225**(1), 203–222 (1997).
- ⁴⁰ W. Liu, and D. Peng, "Exact two-component Hamiltonians revisited," *The Journal of Chemical Physics* **131**(3), 31104 (2009).

- ⁴¹ L. Cheng, and J. Gauss, "Analytic energy gradients for the spin-free exact two-component theory using an exact block diagonalization for the one-electron Dirac Hamiltonian," *Journal of Chemical Physics* **135**(8), (2011).
- ⁴² L. Cheng, and J. Gauss, "Analytic second derivatives for the spin-free exact two-component theory," *The Journal of Chemical Physics* **135**(24), 244104 (2011).
- ⁴³ W. Zou, M. Filatov, and D. Cremer, "Development and application of the analytical energy gradient for the normalized elimination of the small component method," *The Journal of Chemical Physics* **134**(24), 244117 (2011).
- ⁴⁴ W. Zou, M. Filatov, and D. Cremer, "Analytic calculation of second-order electric response properties with the normalized elimination of the small component (NESC) method," *The Journal of Chemical Physics* **137**(8), 084108 (2012).
- ⁴⁵ L. Cheng, F. Wang, J.F. Stanton, and J. Gauss, "Perturbative treatment of spin-orbit-coupling within spin-free exact two-component theory using equation-of-motion coupled-cluster methods," *The Journal of Chemical Physics* **148**(4), 044108 (2018).
- ⁴⁶ P.A.M. Dirac, "The quantum theory of the electron," *Proceedings of the Royal Society of London. Series A, Containing Papers of a Mathematical and Physical Character* **117**(778), 610–624 (1928).
- ⁴⁷ P.A.M. Dirac, "The quantum theory of the electron. Part II," *Proceedings of the Royal Society of London. Series A, Containing Papers of a Mathematical and Physical Character* **118**(779), 351–361 (1928).
- ⁴⁸ K.G. Dyall, and K.F. Jr, *Introduction to Relativistic Quantum Chemistry* (Oxford University Press, 2007).
- ⁴⁹ P. Norman, K. Ruud, and T. Saue, *Principles and Practices of Molecular Properties: Theory, Modeling, and Simulations* (John Wiley & Sons, 2018).
- ⁵⁰ C. Hättig, and F. Weigend, "CC2 excitation energy calculations on large molecules using the resolution of the identity approximation," *The Journal of Chemical Physics* **113**(13), 5154–5161 (2000).
- ⁵¹ M. Feyereisen, G. Fitzgerald, and A. Komornicki, "Use of approximate integrals in ab initio theory. An application in MP2 energy calculations," *Chemical Physics Letters* **208**(5), 359–363 (1993).
- ⁵² E.G. Hohenstein, and C.D. Sherrill, "Density fitting and Cholesky decomposition approximations in symmetry-adapted perturbation theory: Implementation and application to probe the nature of π - π interactions in linear acenes," *The Journal of Chemical Physics* **132**(18), 184111 (2010).
- ⁵³ S.F. Boys, G.B. Cook, C.M. Reeves, and I. Shavitt, "Automatic Fundamental Calculations of Molecular Structure," *Nature* **178**(4544), 1207–1209 (1956).

- ⁵⁴ B.I. Dunlap, J.W.D. Connolly, and J.R. Sabin, "On some approximations in applications of $X\alpha$ theory," *The Journal of Chemical Physics* **71**(8), 3396–3402 (1979).
- ⁵⁵ J.L. Whitten, "Coulombic potential energy integrals and approximations," *The Journal of Chemical Physics* **58**(10), 4496–4501 (1973).
- ⁵⁶ E.G. Hohenstein, R.M. Parrish, and T.J. Martínez, "Tensor hypercontraction density fitting. I. Quartic scaling second- and third-order Møller-Plesset perturbation theory," *The Journal of Chemical Physics* **137**(4), 044103 (2012).
- ⁵⁷ E.G. Hohenstein, S.I.L. Kokkila, R.M. Parrish, and T.J. Martínez, "Quartic scaling second-order approximate coupled cluster singles and doubles via tensor hypercontraction: THC-CC2," *The Journal of Chemical Physics* **138**(12), 124111 (2013).
- ⁵⁸ E.G. Hohenstein, S.I.L. Kokkila, R.M. Parrish, and T.J. Martínez, "Tensor Hypercontraction Equation-of-Motion Second-Order Approximate Coupled Cluster: Electronic Excitation Energies in $O(N_4)$ Time," *J. Phys. Chem. B* **117**(42), 12972–12978 (2013).
- ⁵⁹ A.K. Dutta, F. Neese, and R. Izsák, "Speeding up equation of motion coupled cluster theory with the chain of spheres approximation," *The Journal of Chemical Physics* **144**(3), 034102 (2016).
- ⁶⁰ A.K. Dutta, A. Manna, B. Jangid, K. Majee, K. Surjuse, M. Mukherjee, M. Thapa, S. Arora, S. Chamoli, S. Haldar, S. Chakraborty, and T. Mukhopadhyay, "BAGH: A quantum chemistry software package," (2023).
- ⁶¹ K.U. Lao, J. Jia, R. Maitra, and R.A. DiStasio Jr., "On the geometric dependence of the molecular dipole polarizability in water: A benchmark study of higher-order electron correlation, basis set incompleteness error, core electron effects, and zero-point vibrational contributions," *The Journal of Chemical Physics* **149**(20), 204303 (2018).
- ⁶² T. Saue, R. Bast, A.S.P. Gomes, H.J.Aa. Jensen, L. Visscher, I.A. Aucar, R. Di Remigio, K.G. Dyall, E. Eliav, E. Fasshauer, T. Fleig, L. Halbert, E.D. Hedegård, B. Helmich-Paris, M. Iliaš, C.R. Jacob, S. Knecht, J.K. Laerdahl, M.L. Vidal, M.K. Nayak, M. Olejniczak, J.M.H. Olsen, M. Pernpointner, B. Senjean, A. Shee, A. Sunaga, and J.N.P. van Stralen, "The DIRAC code for relativistic molecular calculations," *The Journal of Chemical Physics* **152**(20), 204104 (2020).
- ⁶³ A.S.P. Gomes, T. Saue, L. Visscher, H.J.Aa. Jensen, R. Bast, I.A. Aucar, V. Bakken, K.G. Dyall, S. Dubillard, U. Ekström, E. Eliav, T. Enevoldsen, E. Faßhauer, T. Fleig, O. Fossgaard, L. Halbert, E.D. Hedegård, T. Helgaker, B. Helmich-Paris, J. Henriksson, M. Iliaš, Ch.R. Jacob, S. Knecht, S. Komorovský, O. Kullie, J.K. Lærdahl, C.V. Larsen, Y.S. Lee, H.S. Nataraj, M.K. Nayak, P. Norman, G. Olejniczak, J. Olsen, J.M.H. Olsen, Y.C. Park, J.K. Pedersen, M. Pernpointner, R. Di Remigio, K. Ruud, P. Sałek, B. Schimmelpfennig, B. Senjean, A. Shee, J. Sikkema, A.J. Thorvaldsen, J. Thyssen, J. van Stralen, M.L. Vidal, S. Villaume, O. Visser, T. Winther, and S. Yamamoto, "DIRAC19," (2019).
- ⁶⁴ J. Olsen, and P. Jørgensen, "Linear and nonlinear response functions for an exact state and for an MCSCF state," *The Journal of Chemical Physics* **82**(7), 3235–3264 (1985).

- ⁶⁵ A. Dreuw, and M. Head-Gordon, "Single-Reference ab Initio Methods for the Calculation of Excited States of Large Molecules," *Chem. Rev.* **105**(11), 4009–4037 (2005).
- ⁶⁶ A.D. McLACHLAN, and M.A. BALL, "Time-Dependent Hartree---Fock Theory for Molecules," *Rev. Mod. Phys.* **36**(3), 844–855 (1964).
- ⁶⁷ R.D. Amos, N.C. Handy, P.J. Knowles, J.E. Rice, and A.J. Stone, "AB-initio prediction of properties of carbon dioxide, ammonia, and carbon dioxide...ammonia," *J. Phys. Chem.* **89**(11), 2186–2192 (1985).
- ⁶⁸ M.J. Jamieson, "Time-dependent hartree–fock theory for atoms," *International Journal of Quantum Chemistry* **5**(S4), 103–115 (1970).
- ⁶⁹ U. Hohm, "Experimental static dipole–dipole polarizabilities of molecules," *Journal of Molecular Structure* **1054–1055**, 282–292 (2013).
- ⁷⁰ U. Hohm, and K. Kerl, "Interferometric measurements of the dipole polarizability α of molecules between 300 K and 1100 K," *Molecular Physics* **69**(5), 803–817 (1990).
- ⁷¹ D. Goebel, U. Hohm, and G. Maroulis, "Theoretical and experimental determination of the polarizabilities of the zinc 1S_0 state," *Phys. Rev. A* **54**(3), 1973–1978 (1996).
- ⁷² U. Hohm, "Dipole–Dipole Polarizability of the Cadmium $1S_0$ State Revisited," *Opt. Spectrosc.* **130**(4), 290–294 (2022).
- ⁷³ D. Goebel, and U. Hohm, "Dispersion of the refractive index of cadmium vapor and the dipole polarizability of the atomic cadmium $1S_0$ state," *Physical Review A* **52**(5), 3691 (1995).
- ⁷⁴ D. Goebel, and U. Hohm, "Dipole polarizability, cauchy moments, and related properties of Hg," *Journal of Physical Chemistry* **100**(18), 7710–7712 (1996).
- ⁷⁵ U. Hohm, "Dipole–Dipole Polarizability of the Cadmium $1S_0$ State Revisited", *Opt. Spectrosc* **130**, 290–294 (2022).
- ⁷⁶ A. Kumar, and W.J. Meath, "Integrated dipole oscillator strengths and dipole properties for Ne, Ar, Kr, Xe, HF, HCl, and HBr," *Can. J. Chem.* **63**(7), 1616–1630 (1985).
- ⁷⁷ C. Cuthbertson, and M. Cuthbertson, "On the Refraction and Dispersion of the Halogens, Halogen Acids, Ozone, Steam, Oxides of Nitrogen and Ammonia," *Philosophical Transactions of the Royal Society of London. Series A, Containing Papers of a Mathematical or Physical Character* **213**, 1–26 (1914).
- ⁷⁸ K.M. Swift, L.A. Schlie, and R.D. Rathge, "Dispersion of gases in atomic iodine lasers at 1.315 μm ," *Appl. Opt.*, **AO** **27**(21), 4377–4384 (1988).
- ⁷⁹ G. Maroulis, C. Makris, U. Hohm, and D. Goebel, "Electrooptical Properties and Molecular Polarization of Iodine, I_2 ," *J. Phys. Chem. A* **101**(5), 953–956 (1997).

⁸⁰ R. Antoine, D. Rayane, A.R. Allouche, M. Aubert-Frécon, E. Benichou, F.W. Dalby, Ph. Dugourd, M. Broyer, and C. Guet, "Static dipole polarizability of small mixed sodium–lithium clusters," *The Journal of Chemical Physics* **110**(12), 5568–5577 (1999).

⁸¹ G. Maroulis, C. Makris, U. Hohm, and D. Goebel, "Electrooptical Properties and Molecular Polarization of Iodine, I₂," *J. Phys. Chem. A* **101**(5), 953–956 (1997).

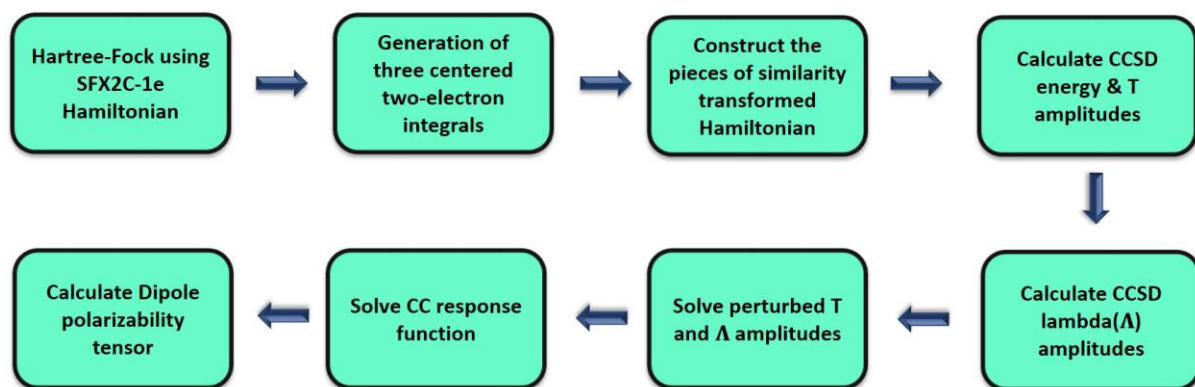


Figure 1: The flowchart for SFX2C1e Linear Response Coupled Cluster theory

Table 1: Benchmarking of basis set for LR-CCSD calculation for Kr atom

Freq	Augmentation	dyall.ae2z	dyall.ae3z	dyall.ae4z	Ref.
0.072	without aug	7.338	12.109	14.548	
0.072	s-aug	16.671	17.108	16.984	
0.072	d-aug	17.314	17.052	16.994	17.075 ⁷⁰
0.072	t-aug	17.321	17.115	16.995	
0.072	q-aug	17.326	17.115	16.995	

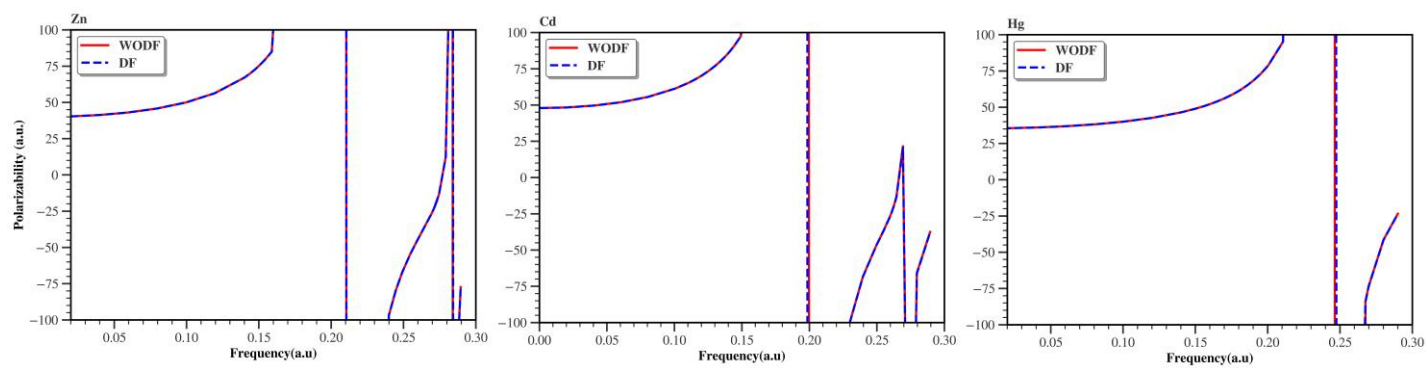


Figure 2: *SFX2C1e-LRCCSD dynamic polarizabilities with (DF) and without density fitting (WODF) for Zn, Cd and Hg*

Table 2: SCF and correlation contribution to the static and dynamic polarizability at *s*-aug-dyall.v2z basis set

Atom	Freq (a.u)	0.0000	0.07198	0.08383	0.14014
Zn	NR-TDHF	53.11	62.29	66.45	126.28
	SFX2C1e-TDHF	49.89	57.87	61.42	108.88
	NR-CC	42.64	47.94	50.20	75.50
	SFX2C1e-CC	39.99	44.57	46.50	67.15
	Expt	38.80(8) ⁷¹	43.03(32) ⁷¹	44.76(31) ⁷¹	63.26(12) ⁷¹
Cd	NR-TDHF	74.91	93.84	103.40	404.86
	SFX2C1e-TDHF	62.79	75.10	80.91	186.14
	NR-LRCC	57.03	66.13	70.22	127.54
	SFX2C1e-LRCC	47.89	53.81	56.36	85.94
	Expt	47.50 ± 2 ⁷²	54.20 ± 0.95 ⁷³	56.23 ± 0.38 ⁷³	68.80 ± 2.3 ⁷³
Hg	NR-TDHF	79.71	100.84	111.80	590.35
	SFX2C1e-TDHF	44.21	48.76	50.68	71.71
	NR-LRCC	59.59	68.87	73.06	132.84
	SFX2C1e-LRCC	35.3278	37.55	38.43	46.42
	Expt	33.92(7) ⁷⁴	35.75(310) ⁷⁴	36.63(317) ⁷⁴	44.64(331) ⁷⁴

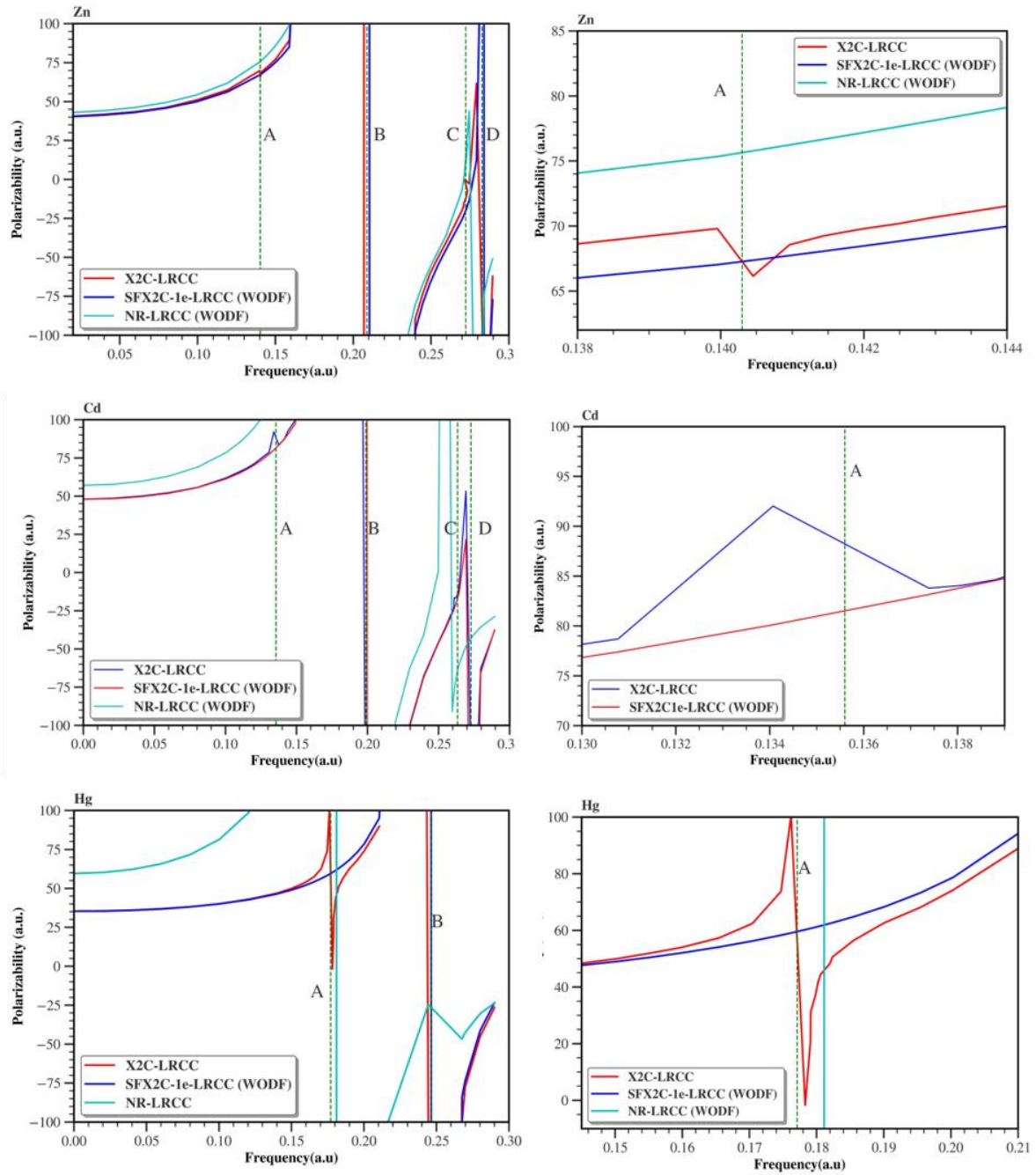


Figure 3: The pole structure of frequency-dependent dynamic polarizabilities (left) and zoomed out version of the pol corresponding to $^1S_0 \rightarrow ^3P_1$ transition. The X2C-LRCC results were taken from reference²⁰

Table 3: Comparison of nonrelativistic, SFX2C1e and X2C LR-CCSD results for static and dynamic polarizability with experiment

Atom	Frequency(a.u.)	SFX2C(a.u.) ^a	NR(a.u.) ^a	X2C(a.u.) ^b	Expt(a.u.)
Zn	0.00000	39.34	41.81	40.42	38.80 ⁷¹
	0.07198	43.74	46.89		43.03 ⁷¹
	0.08383	45.58	49.05		44.76 ⁷¹
	0.14014	65.16	72.98		63.26 ⁷¹
Cd	0.00000	46.81	55.73	48.25	47.50 ⁷⁵
	0.07198	52.40	64.41		54.20 ⁷³
	0.08383	54.79	68.31		56.23 ⁷³
	0.14014	82.05	120.59		68.80 ⁷³
Hg	0.00000	35.04	58.55	35.25	33.92 ⁷⁴
	0.07198	37.22	67.55		35.75 ⁷⁴
	0.08383	37.77	71.61		36.63 ⁷⁴
	0.14014	45.37	128.61		44.64 ⁷⁴

^a s-aug-dyall.ae4z

^b s-aug-dyall.v2z, The X2C-LRCC results were taken from reference²⁰

Table 4: Static polarizabilities of AuH based on SFX2C1e-LRCCSD* and 4C-LR-DFT¹⁶

Method	nX	$\bar{\alpha}$	$\alpha_{ }$	α_{\perp}
SFX2C1e-LRCCSD ^a	2D	36.33	40.29	34.36
	3T	37.31	40.47	35.74
4c-DFT (B3LYP)	uncDZ*	35.67	38.63	34.19
	uncTZ*	36.76	38.99	35.64
4c-DFT (BLYP)	uncDZ*	35.99	38.97	34.50
	uncTZ*	37.15	39.32	36.07
4c-DFT (LDA)	uncDZ*	34.97	37.91	33.49
	uncTZ*	36.36	38.53	35.28

^aAu: dyall.aenz, H: aug-cc-pVXZ

Table 5: Static polarizabilities of diatomic molecules in different level of theories

Molecule	X2C ^a	X2C ^b	SFX2C1e ^c	SFX2C1e ^d	Expt
HF	5.05	5.52	5.58	4.97	5.60±0.10 ⁷⁶
HCl	16.09	17.14	17.34	16.11	17.39±0.20 ⁷⁶
HBr	22.58	24.02	23.82	22.20	23.74±0.50 ⁷⁶
HI	34.30		35.42	34.76	35.30±0.50 ⁷⁷
ICl	47.59		49.18	48.08	43.80±4.40 ⁷⁸
I ₂	69.72		70.53	69.41	69.70±1.80 ⁷⁹
NaLi	240	239	229	236	263±20 ⁸⁰
CsK	611		601	607	601±44 ⁷⁹

a. Relativistic calculation using the full X2C Hamiltonian (s-aug-dyall.v2z)²⁰

b. Using diffuse triple-zeta basis set based on full X2C Hamiltonian²⁰

c. SFX2C1e using d-aug-dyall.v4z basis set (This work)

d. SFX2C1e using s-aug-dyall.v2z basis set (I, Cs) and unc-aug-cc-PVDZ (H, F, Cl, Br) (This work)

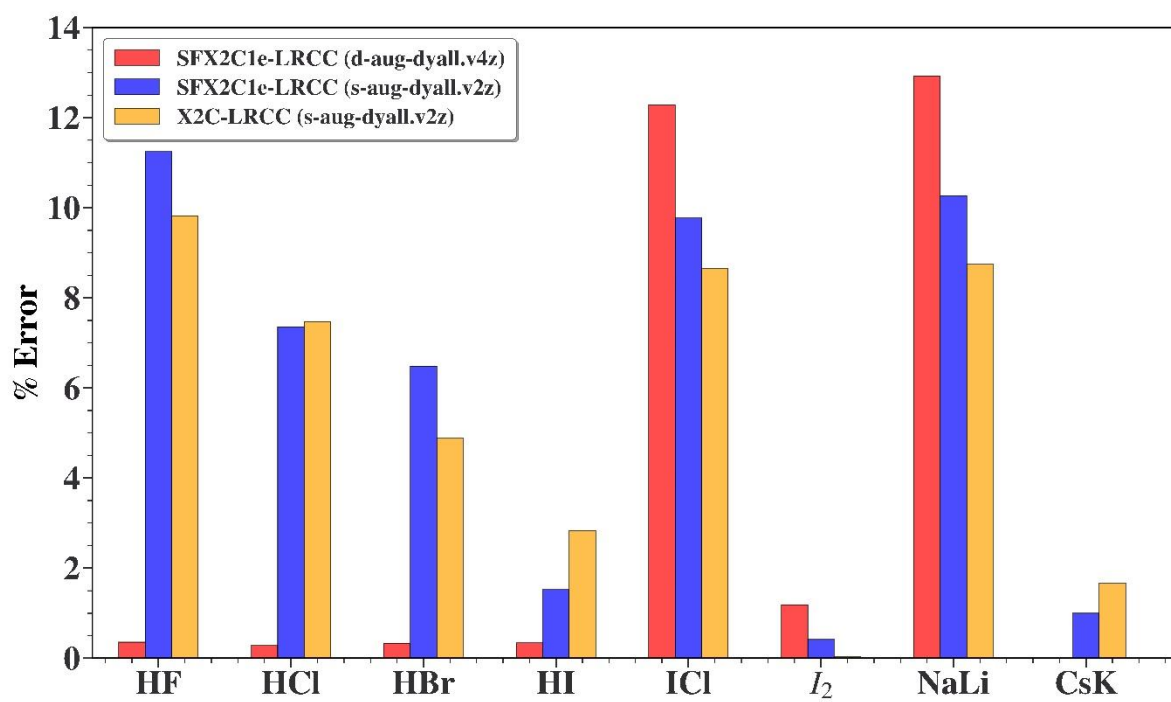


Figure 3: Error in static polarizability with respect to the experiments

Table 6: Dynamic polarizabilities of Iodine Dimer (I_2)

	$\alpha_{xx}(\omega)$	$\alpha_{zz}(\omega)$	$\alpha(\omega)$
Frequency = 0.07198 a.u.			
SFX2C1e-LRCCSD	58.55	104.14	73.8
X2C-HF ^{a20}	55.0	152.0	87.4
B3LYP ^{a20}	58.7	-10.7	35.6
X2C- LRCCSD ^{a20}	55.8	114.8	75.5
Expt ⁸¹			86.8 \pm 2.2
Frequency = 0.07669 a.u.			
SFX2C1e-LRCCSD	59.1	104.8	74.3
X2C-HF ^a	56.0	-97.3	4.9
B3LYP ^a	62.0	75.4	66.5
X2C- LRCCSD ^a	56.8	124.0	79.2
Expt ⁸¹			93.6 \pm 3.4
Frequency = 0.14014 a.u			
SFX2C1e-LRCCSD	62.4	121.2	82.0
X2C-HF ^a	55.3	117.9	76.2
B3LYP ^a	61.0	114.5	78.8
X2C- LRCCSD ^a	59.9	113.9	77.9
Expt ⁸¹			95.3 \pm 1.9

^a HF, X2C and B3LYP results are taken from Yuan *et al.*²⁰

Table 7: Static polarizabilities (a.u.) of UF_6 , OsO_4 and $HgCl_2$

molecule	Method	$\alpha_{xx}(\omega)$	$\alpha_{yy}(\omega)$	$\alpha_{zz}(\omega)$	$\alpha(\omega)$
UF_6	SFX2C1e-LRCCSD ^a	52.39	52.39	52.39	52.39
	NESC/PBE0 ⁴⁴	51.35	51.35	51.35	51.35
	NESC/MP2 ⁴⁴	54.19	54.19	54.19	54.19
	Experiment ⁶⁹				83.02 ± 0.5
OsO_4	SFX2C1e-LRCCSD ^a	52.45	52.45	52.45	52.45
	NESC/PBE0 ⁴⁴	46.50	46.50	46.50	46.50
	NESC/MP2 ⁴⁴	55.54	55.54	55.54	55.54
	Experiment ⁶⁹				55.1 ± 0.8
$HgCl_2$	SFX2C1e-LRCCSD ^a	42.10	42.10	80.21	54.80
	NESC/PBE0 ⁴⁴	40.76	40.76	91.91	57.83
	NESC/MP2 ⁴⁴	40.42	40.42	93.26	58.03
	Experiment ⁶⁹				78.2 ± 1

^aSARC-DKH: U, Os, Hg, def2-QZVPP: F, O, Cl

**Supplementary information: Spin-free exact two-component linear response
coupled cluster theory for estimation of frequency-dependent second-order
property**

Sudipta Chakraborty^a, Tamoghna Mukhopadhyay^a and Achintya Kumar Dutta^{*,a}

^aDepartment of Chemistry, Indian Institute of Technology Bombay, Mumbai 400076, India

**achintya@chem.iitb.ac.in*

Table S1: Static and dynamic polarizabilities of Group-2 elements

Atom	Freq	SFX2C-1e-LR ^a	SFX2C1e-LR ^b	Ref
Be	0.070	43.29	43.68	43.26 ¹
Mg	0.000	71.38	71.42	71.5±3.5 ²
Ca	0.000	156.37	156.12	169±17 ³
Sr	0.000	196.06	195.76	186±15 ⁴
Ba	0.000	269.47	270.09	268±22 ³
Ra	0.000		245.75	236±15 ^{5*}

^a t-aug-dyall.ae3z

^b s-aug-dyall.ae4z

*R, CCSD(T)

Table S2: Static and dynamic polarizabilities of Group-18 elements

Atom	Freq	SFX2C-1e-LR ^a	SFX2C-1e-LR ^b	Ref
He	0.072	1.388	1.380	1.383759±0.000013 ⁶
Ne	0.072	2.705	2.617	2.66110±0.00003 ⁷
Ar	0.072	11.333	11.137	11.070±0.007 ⁸
Kr	0.072	17.115	16.984	16.782±0.005 ⁹
Xe	0.072	27.85	27.57	27.078±0.050 ⁹
Rn	0.000		33.09	35.04±1.8 ^{10*}

^at-aug-dyall.ae3z

^bs-aug-dyall.ae4z

*R, Dirac, CCSD(T)

- *Cartesian coordinates of the molecules considered in this manuscript:*

Hydrogen Fluoride:

H	0.00000	0.00000	0.00000
F	0.00000	0.00000	0.91680

Hydrogen Chloride:

H	0.00000	0.00000	0.00000
Cl	0.00000	0.00000	1.27450

Hydrogen Bromide:

H	0.00000	0.00000	0.00000
Br	0.00000	0.00000	1.41440

Hydrogen Iodide:

H	0.00000	0.00000	0.00000
I	0.00000	0.00000	1.60916

Iodine monochloride:

H	0.00000	0.00000	0.00000
F	0.00000	0.00000	2.32087

Iodine dimer:

I	0.00000	0.00000	0.00000
I	0.00000	0.00000	2.66630

Na-Li:

Na	0.00000	0.00000	0.00000
Li	0.00000	0.00000	2.81000

K-Cs:

K	0.00000	0.00000	0.00000
Cs	0.00000	0.00000	4.28500

Gold Hydride(AuH):

H	0.00000	0.00000	0.00000
Au	0.00000	0.00000	1.52850

Mercury(II) Chloride:

Hg	0.00000	0.00000	0.00000
Cl	0.00000	0.00000	2.28000
Cl	0.00000	0.00000	-2.28000

Osmium Tetraoxide:

O	0.00000	0.00000	0.00000
Os	1.71400	0.00000	0.00000
O	2.28534	1.61597	0.00000
O	2.28533	-1.39947	-0.80800
O	2.28533	1.39948	-0.80798

Urenium Hexafluoride (UF₆):

U	0.00000	0.00000	0.00000
F	0.00000	0.00000	1.99900
F	0.00000	0.00000	-1.99900
F	0.00000	1.99900	0.00000
F	0.00000	-1.99900	0.00000
F	1.99900	0.00000	0.00000
F	-1.99900	0.00000	0.00000

References

- ¹ J. Komasa, “Dipole and quadrupole polarizabilities and shielding factors of beryllium from exponentially correlated Gaussian functions,” *Phys. Rev. A* **65**(1), 012506 (2001).
- ² L. Lundin, B. Engman, J. Hilke, and I. Martinson, “Lifetime Measurements in Mg I-Mg IV,” *Phys. Scr.* **8**(6), 274 (1973).
- ³ H.L. Schwartz, T.M. Miller, and B. Bederson, “Measurement of the static electric dipole polarizabilities of barium and strontium,” *Phys. Rev. A* **10**(6), 1924–1926 (1974).
- ⁴ D.R. Lide, *CRC Handbook of Chemistry and Physics* (CRC press, 2004).
- ⁵ B.K. Sahoo, and B.P. Das, “The role of relativistic many-body theory in probing new physics beyond the standard model via the electric dipole moments of diamagnetic atoms,” *J. Phys.: Conf. Ser.* **1041**(1), 012014 (2018).
- ⁶ J.W. Schmidt, R.M. Gaviolo, E.F. May, and M.R. Moldover, “Polarizability of Helium and Gas Metrology,” *Phys. Rev. Lett.* **98**(25), 254504 (2007).
- ⁷ C. Gaiser, and B. Fellmuth, “Experimental benchmark value for the molar polarizability of neon,” *EPL* **90**(6), 63002 (2010).
- ⁸ U. Hohm, and K. Kerl, “Interferometric measurements of the dipole polarizability α of molecules between 300 K and 1100 K: I. Monochromatic measurements at $\lambda = 632.99$ nm for the noble gases and H₂, N₂, O₂, and CH₄,” *Molecular Physics* **69**(5), 803–817 (1990).
- ⁹ J. Huot, and T.K. Bose, “Experimental determination of the dielectric virial coefficients of atomic gases as a function of temperature,” *The Journal of Chemical Physics* **95**(4), 2683–2687 (1991).
- ¹⁰ U. Hohm, and A.J. Thakkar, “New Relationships Connecting the Dipole Polarizability, Radius, and Second Ionization Potential for Atoms,” *J. Phys. Chem. A* **116**(1), 697–703 (2012).